Journal of Petroleum Exploration and Production Technology (2020) 10:2575–2585
https://doi.org/10.1007/s13202-020-00899-0

ORIGINAL PAPER - PRODUCTION ENGINEERING

Feasibility of miscible CO_2 flooding in hydrocarbon reservoirs with different crude oil compositions

Mudassir Khan[1] · Arshad Raza[1] · Muhammad Khurram Zahoor[1] · Raoof Gholami[2]

Received: 25 February 2020 / Accepted: 28 April 2020 / Published online: 8 May 2020

Abstract

Miscible CO_2-based enhanced oil recovery (CO_2-EOR) flooding has been used, on many occasions, to maximize the recovery by mobilizing the residual oil. The success of this method, however, depends highly on the minimum miscibility pressure (MMP), the compatibility of CO_2 with the reservoir rock and fluids. Although there have been several studies on the application of CO_2-EOR, the impact of oil compositions associated with MMP on the feasibility of this technique has not been addressed elsewhere. In this study, a simulation study was carried out to investigate the effect of three different oil compositions on the miscibility and ultimate oil recovery of miscible CO_2-EOR method. The results obtained indicated the oil type does not pose a significant impact on the success of miscible CO_2-EOR. It was also found that the ultimate recovery of oil increases in a short period of time by injecting CO_2 at the miscible conditions at the early stage of natural production. Comparatively, the reservoir with the fluid sample S2 seems to be a suitable choice for the miscible CO_2 flooding once the recovery factor was considered together with the total amount of the fluid injected and produced.

Keywords Simulation · Miscible flooding · CO_2-EOR · Oil composition · Recovery

Introduction

Natural depletion of hydrocarbon reservoirs often does exceed 20% to 40% in the primary recovery phase (Orr et al. 1982; Muggeridge et al. 2014; Raza et al. 2019). As a result, certain EOR methods such as gas, chemical or thermal injections are used for production enhancement (Muggeridge et al. 2014). Given the characteristics of CO_2, it is comparatively considered as one of the best option of gas injection during the tertiary recovery stage (Bachu 2016).

CO_2 injection is done under the miscible or immiscible phases depending on the minimum miscibility pressure (MMP) (Gao et al. 2013). This MMP depends on a variety of different parameters including the purity of CO_2, reservoir pressure, and temperature as well as the composition of the reservoir oil. Some other factors such as the pressure, residence time, slug size, and fluid properties (i.e., surface tension, density, viscosity, and purity) have also been indicated as the major parameters controlling the miscibility of injected CO_2 (Kurdi et al. 2012; Choubineh et al. 2019; Bhatti et al. 2018). There have also been different mechanisms suggested as the reason behind the increase in ultimate recovery in the miscible CO_2 injection process which include: (1) oil swelling, (2) oil viscosity reduction, (3) mobility ratio reduction, (4) interfacial tension reduction, (5) vaporization of light oil component, (6) weak acid impact, and (7) solution gas drive (Mangalsingh and Jagai 1996) as shown in Fig. 1.

Many studies have been done to understand the oil recovery enhanced posed by the miscible CO_2 injection using experimental and numerical simulation approaches. For example, Huang (1992) performed a number of experiments to determine the minimum miscibility pressure by the slim-tube experiments of West Texas crude oil. The calculated MMP was 2150 psi, and Berea core sample was flooded by CO_2 at 2500 psi. It was observed that CO_2 was not miscible with the oil, and miscible core flooding was not achieved even at a higher pressure than MMP (Huang 1992). Izgec et al. (2005) performed an experimental study on the miscible CO_2 injection in carbonate reservoirs. The effects of the chemical changes that occurred due to CO_2 injection

✉ Arshad Raza
Arshadraza212@gmail.com

1 Department of Petroleum & Gas Engineering, University of Engineering and Technology (UET), Lahore, Pakistan

2 Department of Petroleum Engineering, Curtin University, Miri, Malaysia

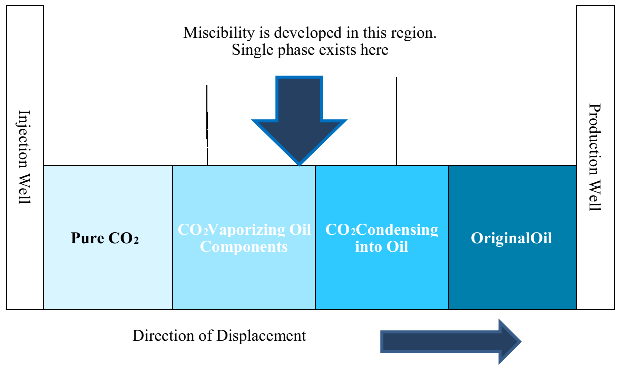

Fig. 1 Miscible CO_2 displacement process

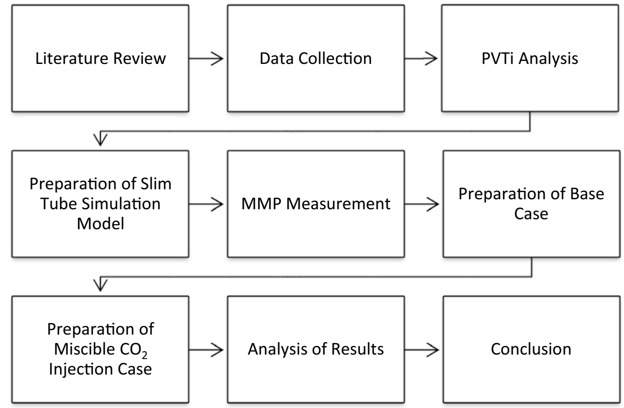

Fig. 2 Research methodology layout used in this study

were studied by the computerized tomography (CT) method. It was observed that the permeability of the reservoir initially increases and then decreases for slow injection rates while calcite scaling was influenced by the direction of flow. Nasir and Amiruddin (2008) developed a simulation model to check the sensitivities of the fluid properties on the miscible CO_2 injection. For this purpose, the effects of different fluid properties such as the density of oil and injected gas, formation volume factor, and viscosity were analyzed. The results obtained indicated that the success of the miscible CO_2 injection depends on the properties of the injected gas and recovered oil. Moreover, the formation volume factor has a significantly higher impact on the ultimate recovery than the density of oil (Nasir and Amiruddin 2008). Abbasi et al. (2010) performed an experimental study on the core samples of an Iranian reservoir. Different percentages of CO_2 gas were injected into the core samples at different injection pressures. The increment in the recovery factor was observed with the increase in the injection pressure close to the miscible conditions. It was shown that the incremental percentage of CO_2 helps to achieve the miscible condition, and the value of the minimum miscibility pressure (MMP) decreases as the percentage of CO_2 increases (Abbasi et al. 2010). Chen et al. (2018) presented different CO_2 injection schemes such as continuous CO_2 flooding, water alternating gas, and carbonated water injection. It was observed that under the miscible condition, the performance of CO_2 EOR reduces due to the presence of initial gas. Thus, it was recommended to go for CO_2–water injection flooding when the initial gas saturation is low (Chen et al. 2018). Bhatti et al. (2018) assessed one of the oil reservoirs in Pakistan for miscible CO_2 injection. It was revealed that the continuous CO_2 and CO_2-water alternating gas (CO_2-WAG) injection give a very high recovery than the primary recovery. In the tertiary recovery stage though, CO_2-WAG was found as the most suitable method given its significant recovery of 200% (Bhatti et al. 2018). Likewise, Chen et al. (2019) performed different experiments in the laboratory to implement the miscible CO_2-EOR technique at an Indian oil field. They indicated that implementation of the miscible CO_2-EOR could improve oil production while reducing CO_2 emission in the atmosphere. Having said that, the feasibility of different oil reservoirs for a successful miscible CO_2 flooding has not been deeply addressed yet. Moreover, the effect of the oil composition/API on the MMP has not been properly studied at the reservoir scale.

In this study, attempts are made to numerically assess the feasibility of different oil reservoirs for the miscible CO_2 flooding. Three oil samples with different APIs were considered ranging from 22.5° to 33.8° API. The results presented as part of this study help to understand the importance of MMP in the selection of oil reservoirs and the injection strategy.

Methodology

The main objective of this study was to analyze the effect of different oil compositions on the minimum miscibility pressure and injection strategy of the CO_2-EOR technique. Figure 2 shows the methodological layout used in this study. Different compositions of light, medium, and heavy oil reported in the literature (McCain Jr 1994; McCain 1990) were considered as given in Table 1. PVTi analysis was, however, performed to measure the physical properties of these fluids. A simulation model of the slim-tube experiment was then used to measure the MMP for each fluid. Three reservoir models were developed for each fluid sample to simulate the natural depletion of the reservoirs. Each simulation was upgraded by incorporating the miscible CO_2 injection technique. Two cases were generated for different injection schemes. In the first injection scheme, CO_2 gas injection was started after the natural depletion of the reservoir (Case 1). In the second injection scheme, CO_2 gas injection was started from the first day of natural production (Case 2).

Table 1 Compositional analysis of three oil samples

S1-composition of oil sample of API 22.5°			S2-composition of oil sample of API 28.7°			S3-composition of oil sample of API 33.8°		
Components	Mole %	Molecular weight	Components	Mole %	Molecular weight	Components	Mole %	Molecular weight
CO_2	2.8	44.01	CO_2	1.17	44.01	CO_2	1.59	44.01
N2	2.54	28.01	N2	0	28.01	N2	0	28.01
C1	24.58	16.04	C1	16.87	16.04	C1	34.28	16.04
C2	4.51	30.07	C2	4.56	30.07	C2	7.52	30.07
C3	3.08	44.09	C3	5.05	44.09	C3	5.64	44.09
IC4	0.87	58.12	IC4	1.66	58.12	IC4	0.97	58.12
NC4	1.48	58.12	NC4	4	58.12	NC4	2.49	58.12
IC5	0.86	72.15	IC5	2.07	72.15	IC5	1.1	72.15
NC5	1.43	72.15	NC5	3.63	72.15	NC5	1.41	72.15
C6	2.31	84.0	C6	4.19	84.0	C6	1.97	84.0
C7+	55.54	230	C7+	56.8	217	C7+	43.03	215
Total	100	–	Total	100	–	Total	100	–

A comparative analysis was then performed based on the results obtained to select a feasible injection plan.

Data sources and model setup

As it was mentioned earlier, three fluid samples with different compositions and API gravity were considered as part of this study as reported in Table 1. Fluid properties were calculated using the PVTi module of Schlumberger Eclipse (E300) software based on the reservoir pressure of 2315 psi and the temperature 149 °F. The pressure–temperature (phase) diagram was then plotted as shown in Fig. 3. This figure shows the phase behavior of the reservoir oil, bubble point pressure, and the percentage of the liquid and gas below the bubble point pressure. Black oil and volatile oil reservoirs fall in this region on the left side of the critical point. It appeared that the bubble point pressure of the samples S1, S2, and S3 would be 1675 psi, 867 psi, and 2057 psi, respectively. Figure 4 shows the calculated formation volume factor, solution gas–oil ratio, and oil viscosity of S1, S2, and S3, and the effect of compositions on PVT properties is evident. S3 is high energy oil with high solution gas–oil ratio compared to S1 and S2 samples. Formation volume factor and solution gas–oil ratio trends of S1 and S2 show the difference before and after bubble point pressure. The trend of viscosity against API is inverse, while trend of viscosity against pressure is typical that decreases till bubble point pressure and then starts to increase.

Binary interaction coefficient was used in the Peng-Robinson equation of state to accounts for the effect of the polar forces in the interaction between components. This equation of state was also used in the numerical simulation model for the calculation of the minimum miscibility pressure. Three-phase diagrams which is also known as the ternary diagram was then plotted as shown in Fig. 5. The envelope in the diagram shows a two-phase region, and the black point shows the composition of the samples. Thus, any line crossing the two-phase envelope shows the immiscibility of the gas in the oil. If the connecting lines do not pass the phase envelope, it shows the complete miscibility of the gas in the oil.

Minimum miscibility pressure calculation was done after the calculation of the fluid properties and parameters used in the Peng–Robinson equation of state. In this study, a simulation method was adopted for the calculation of MMP by Eclipse E300. The simulation was run for a series of different pressures. The recovery factor corresponding to each pressure value was then recorded. A graph was plotted between the pressure values on the *x*-axis and the oil recoveries at the *y*-axis. The break in the curve gives the value of the minimum miscibility pressure. Figure 6 shows the graph of the minimum miscibility pressure.

The relative permeability values were calculated using the Baker model (Baker 1988). Figure 7 shows the relative permeability and the saturation data used in this study at 0.65% oil saturation and 0.35 gas saturation. These values of the oil saturation and gas saturation become 50% and 55%, respectively, after the natural depletion stage. A numerical simulation model was then developed to observe the effect of the composition on the minimum miscibility pressure and the injection strategies. The data used to create the reservoir for the simulation model are reported in Table 2.

As discussed earlier, two injection schemes were adopted in this study for different oil reservoirs to assess the performance of the miscible CO_2 flooding. Given these two cases and three oil samples, a total number of six simulations were run by keeping all the parameters constant except the composition of oils. Figure 8 shows the reservoir model developed for this study with one injection and five production wells. The injection rate was kept constant, and CO_2 gas was

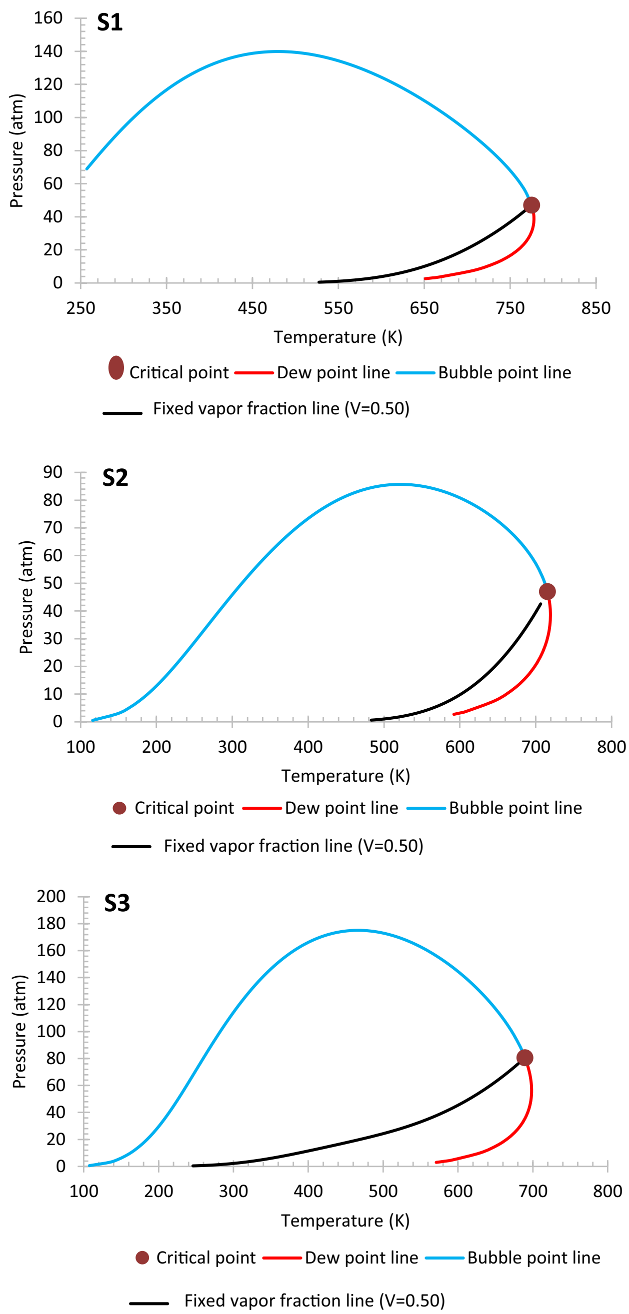

Fig. 3 Schematic two-phase diagrams of three oil samples used in this study

injected in the upper layer, while the production well was completed in the lower structure.

Results and discussion

This section explains the results obtained from the methodology proposed earlier. The results are categorized into the following three categories of: (1) primary recovery, (2) miscible CO_2 injection, and (3) ultimate oil recoveries from two different injection schemes. The base case involves the natural depletion of the reservoir to the economic limit of the reservoir. In the second case, CO_2 is injected in the reservoir above the specific minimum miscibility pressure from the very first day. In the third case, CO_2 injection is started after the natural depletion of the reservoir. At the end, a comparative analysis was performed to select a suitable injection scheme from these two cases. Table 3 gives different development schemes used in the base, first, and second cases.

Primary recovery (base case)

In the base case, the reservoir produces from its natural energy. The solution gas drive mechanism was involved, and the reservoir pressure was already lesser than the bubble point pressure (free gas is present). As the production starts, the pressure of the reservoir starts to deplete, and free gas maintains the reservoir pressure. Figure 9a shows the oil recovery efficiency (FOE) trend against time for sample S1, S2, and S3. It was observed that only 23% to 24% of oil can be recovered from the natural energy in all cases. Thus, an external drive mechanism is required to produce the rest of oil from the reservoir. Figure 9b shows the oil production rate (FOPR) and reservoir pressure (FPR) for 15 years for sample S1, S2, and S3. For S1 and S2, the reservoir pressure declines with oil production after 15 years. Thus, an external energy is required for further production. This reservoir is considered as a suitable choice for the miscible CO_2-EOR.

Case 1: injection from the first day of production

In this case, a reservoir model was developed to incorporate miscible CO_2 injection into the base case from the first day of production. The injection pressure of CO_2 was kept above the minimum miscibility pressure, exceeding the threshold of the initial reservoir pressure to maintain the miscible conditions throughout the reservoir. CO_2 gas becomes miscible in the reservoir by the multi-contact miscibility as a result of vaporization and condensation drive mechanism. Thus, a miscible front of CO_2 and oil was developed in the reservoir which could sweep oil out toward the production well. Figure 10a shows a comparison between the oil production rate (FOPR) and reservoir pressure (FPR) obtained from all three samples.

More pressure buildup was observed in the reservoir with the sample S1 due to a high MMP and a higher injection rate compared to other cases. On the other hand, the reservoir with the sample S3 had a higher MMP than S2. Thus, the pressure rate curve for S3 is between the reservoir with the sample S1 and S2. The fluid sample S2 had the lowest MMP value and attains the miscibility conditions earlier than the other two samples. Similarly, a higher oil production rate

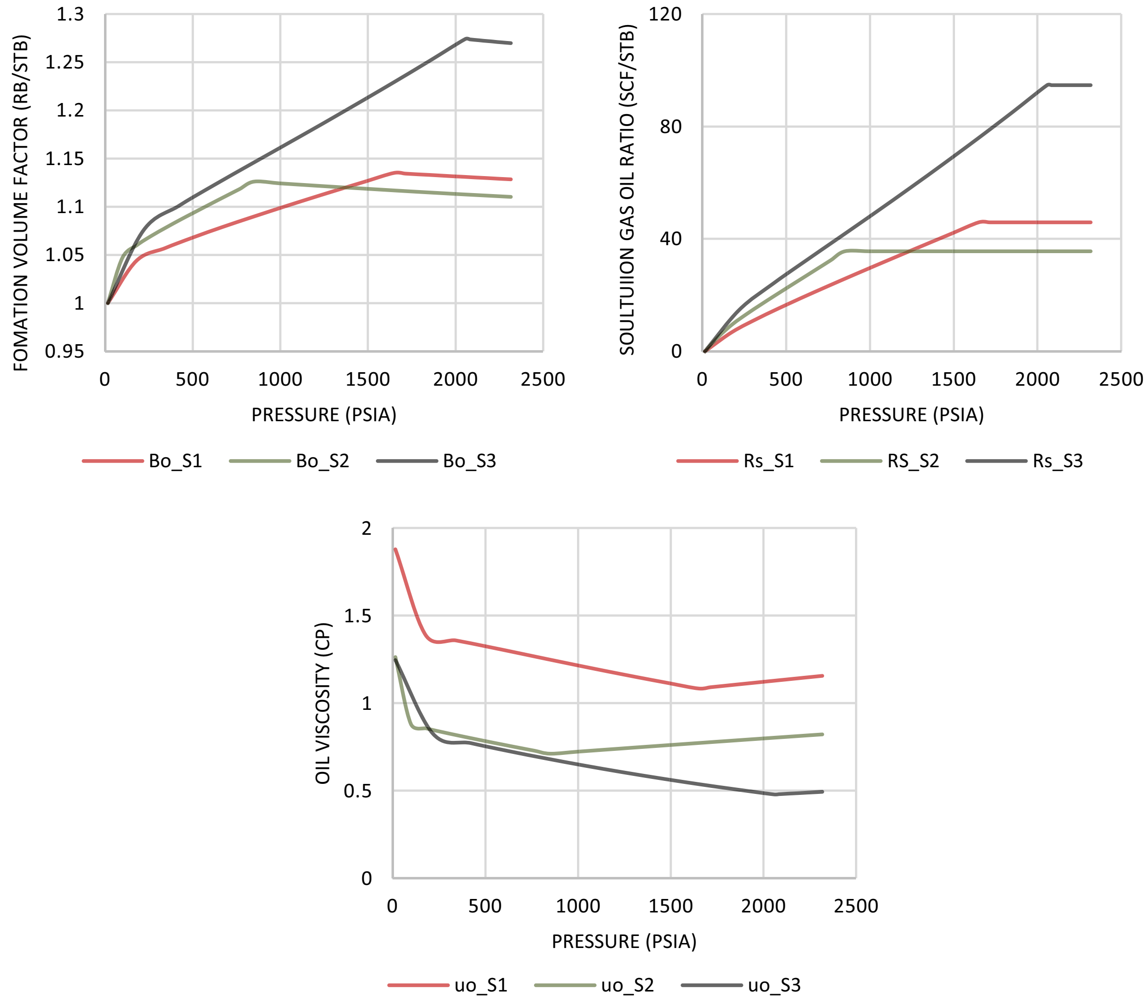

Fig. 4 Calculated formation volume factor, solution gas–oil ratio and oil viscosity of S1, S2 and S3

was observed in the reservoir with the sample S1 due to the high gas injection rate. It was also seen that the reservoir recovery with these fluid samples is almost the same despite their different fluid compositions. Similarly, the oil production rates and cumulative CO_2 production from each case were close because different fluid compositions did not have a significant impact on the total recovery. However, due to different percentages of light and heavy components in the samples, changes in the pressure buildup and gas production rate were clearly observed. Figure 10b compares the gas injection rate (FGIR) and gas production rate (FGPR) obtained from all three cases. As it is seen, at the beginning of production, a higher gas injection rate was selected to maintain the miscible conditions in the reservoirs. Once the MMP is achieved, the gas injection rate was reduced to maintain the reservoir pressure above the MMP. A lowest gas injection rate was, however, selected for the sample S2 due to its lower MMP. A total volume of 569 MMScf gas was injected into the reservoir with sample S3 while 599 MMScf gas was injected for the sample S1 due to its higher MMP. Correspondingly, gas production rates at the end of the production period remain constant Fig. 10c compares the oil recovery efficiency (FOE) and the total fraction of CO_2 production (FZMF1) obtained from all three cases. Apparently, the ultimate recoveries are almost the same for all three samples. However, slightly higher oil recovery efficiency (FOE) was observed in the sample S3 since it contains more fraction of light components with higher fraction of methane. At the end, a total recovery of 79% was achieved in the sample S3 while the remaining two sample (S1 and S2) had the recovery of 78%. It was also noted that the fraction of CO_2 is higher in the sample S1 due to the gas channeling and fingering effect. As the mobility difference between the injected gas and sample S1 is high, a slight fraction of gas passes through the oil and will be produced at the surface. On the other hand, more delay of gas break through was observed in the reservoir with sample S2 due to less amount of gas injection and early attainment of the

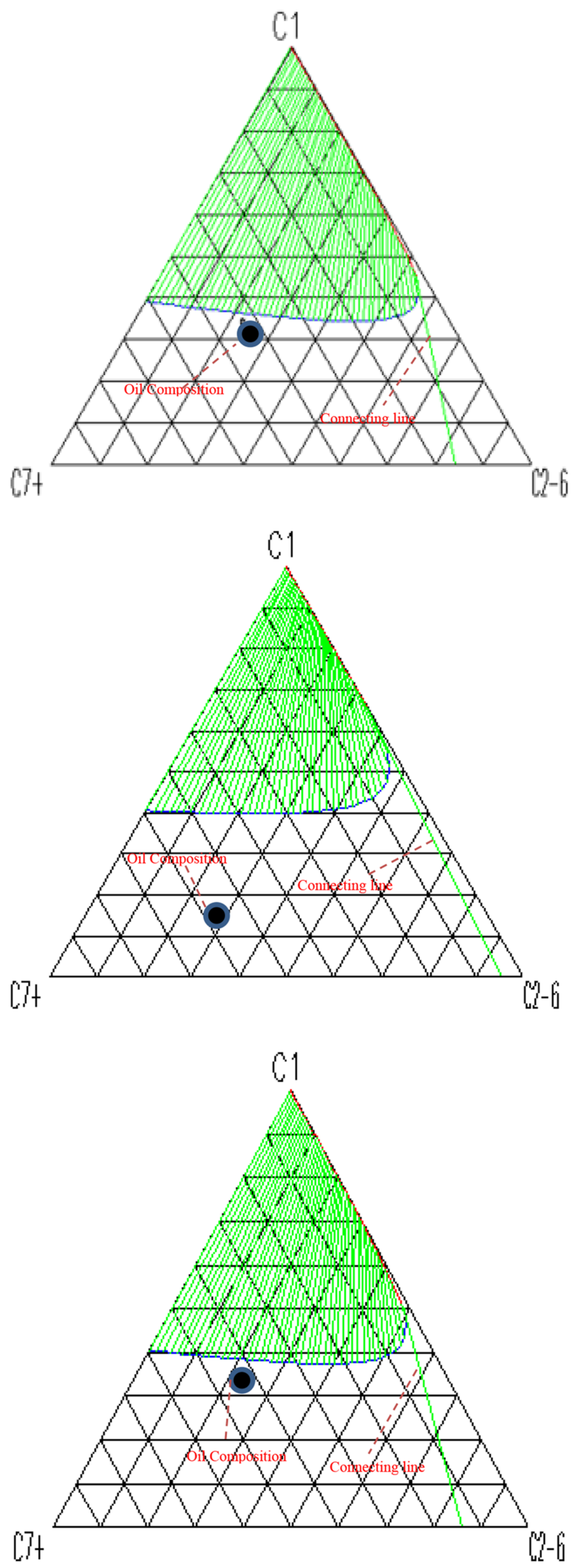

Fig. 5 Schematic ternary diagram for SI (top), S2 (middle) and S3 (bottom) oil samples

MMP. Figure 10d compares the total oil production volumes (FOPT) obtained for all fluid samples. It was revealed that the reservoir with the fluid sample S2 can produce a higher volume of oil than the other reservoirs because of its low MMP and miscibility conditions.

Case 2: injection after natural depletion

In this scenario, miscible CO_2 injection was initiation when almost 75% oil was still left in the reservoir. In this case, the miscibility was achieved by maintaining the injection pressure of CO_2 above the minimum miscibility pressure. Figure 11a plots the oil production rate (FOPR) and reservoir pressure (FPR) against time for the reservoirs with different fluid samples.

More pressure buildup was observed in the S2 reservoir due to the early attainment of MMP and presence of free CO_2 gas in the reservoir. Similarly, the reservoir with the fluid sample S1 gave a higher oil production rate due to the high gas injection volume and rate than the other fluid samples. Figure 11b shows the variation of the gas injection rate (FGIR) and gas production rate (FGPR) against time in all three cases. The residual oil in the reservoir contains more fraction of heavy components and as such more gas is required to produce the residual oil. Similarly, the reservoir with S1 requires a large amount of injected gas for production. Figure 11c plots the oil recovery efficiency (FOE) and the total fraction of CO_2 production (FZMF1) against time in all three fluid samples. There is not a significant difference in the recovery of different cases; however, the reservoir with sample S1 had a higher FOE compared to S2 and S3 that could be due to the favorable fluid displacement. The injected gas reduces the oil viscosity and gas condensation drive increases the mobility of oil and oil produces at the production wells. The mobility difference between the injected gas and the oil samples may lead to CO_2 bypassing and production at the surface. Figure 11d plots the total oil production volumes (FOPT) against time in all three fluid samples. It appears that the reservoir with sample S1 performs better than S2 and S3 due to the higher injected gas volume. The fluid sample S3 had the lowest oil production volume due to a higher fraction of heavy components in the residual oil.

Overall comparison

Table 4 summarizes the results obtained from all the cases generated in this study. It was revealed that miscible CO_2 injection is a suitable technique for the reservoir under consideration, but the main objective of the study was to select the most suitable injection scheme that could increase the recovery in a short time period. It appears that the case-1 in

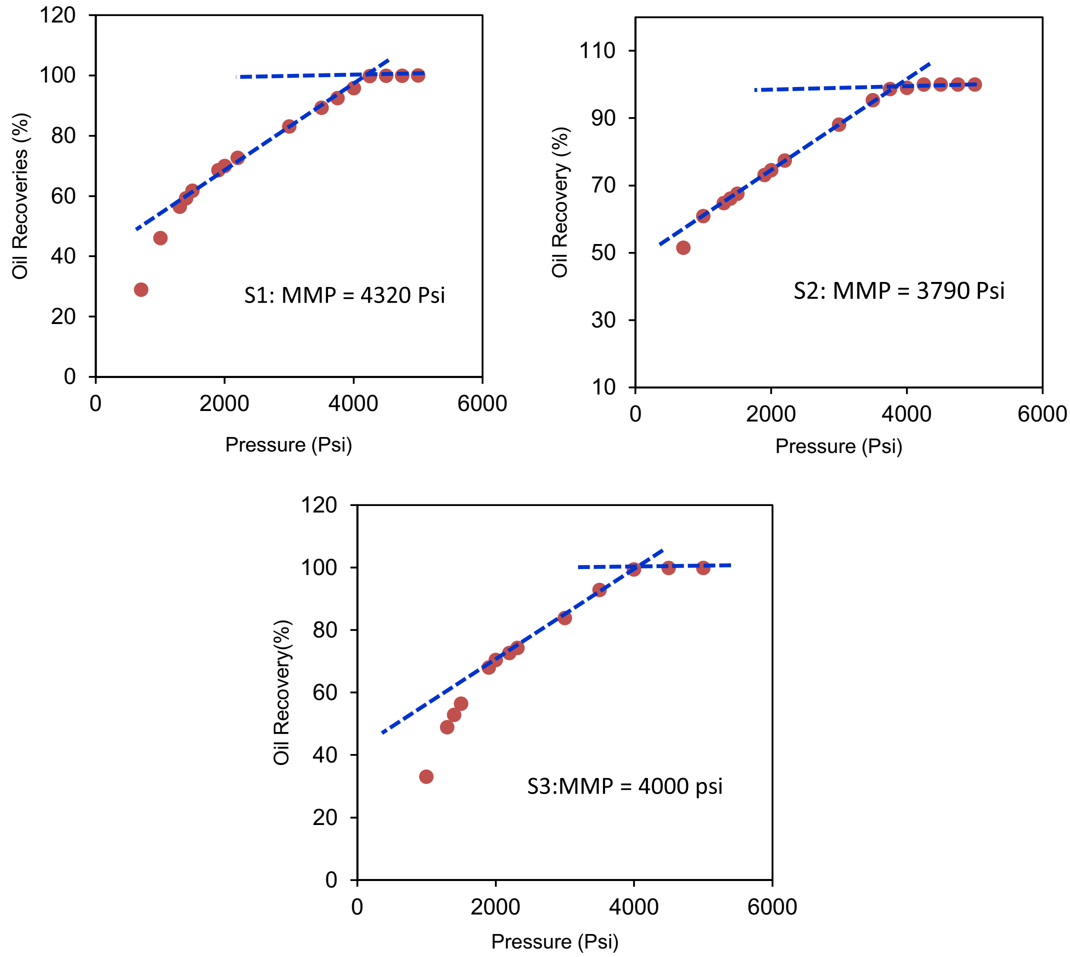

Fig. 6 Oil recovery versus pressure in different fluid samples

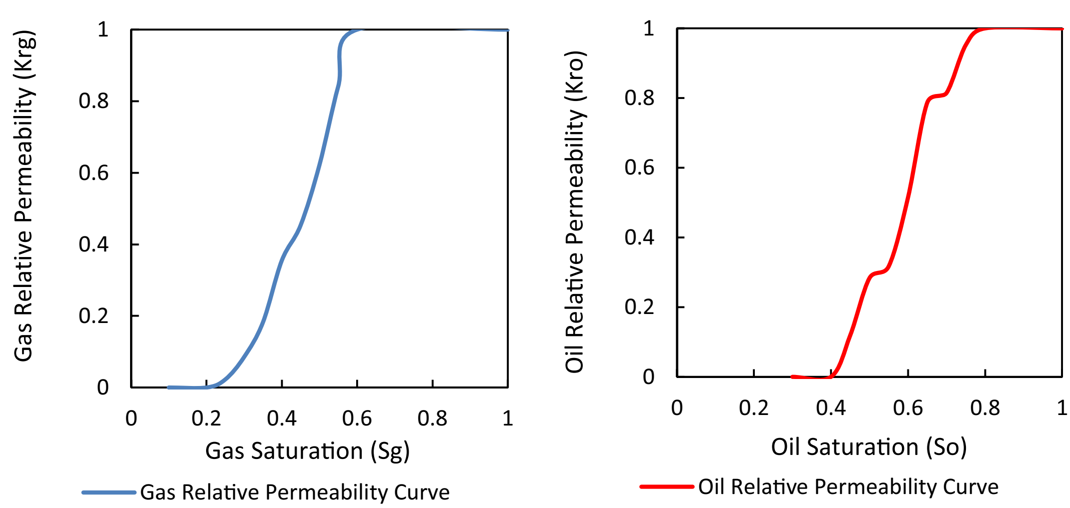

Fig. 7 Relative permeability curves used in this study

Table 2 Hypothetical reservoir data used to build the numerical model

Parameters	Values
Grid blocks	200
No of injection wells	01
No of production wells	04
Permeability	100 mD
Porosity	0.3
Thickness	20 ft
Depth (ft)	3040
Initial OIP (MMSTB)	90
Initial oil saturation (%)	100
Heterogeneity	Homogenous
Reservoir temperature	149 °F
Reservoir pressure	2315 psi
No of components	11
Injected gas	Carbon dioxide (CO_2)

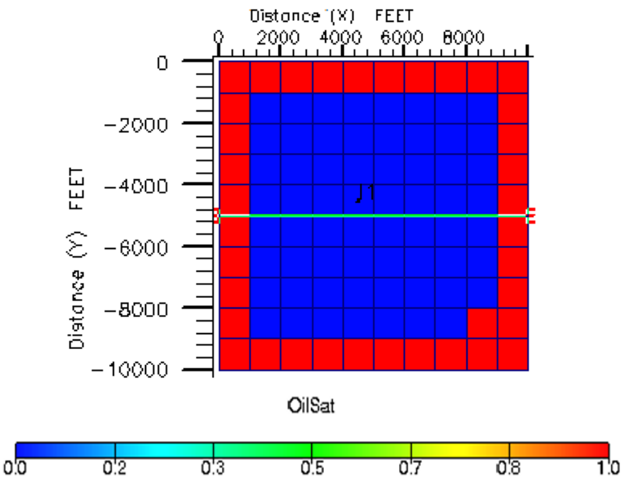

Fig. 8 Hypothetical model (top layer) of the base case reservoir showing the variation of saturation after 15 years of production

Table 3 Different development schemes

Case	Oil API	Injection stage
Base	22.5	Primary recovery
	28.7	
	33.8	
1	22.5	Injection from 1st day of production
	28.7	
	33.8	
2	22.5	Injection after natural depletion of the reservoir
	28.7	
	33.8	

the reservoirs with the S2 fluid sample would be the most suitable scheme where CO_2 injection starts from the very first day of production. It was also seen that the reservoir with the S2 fluid sample gives the maximum recovery with lesser injected gas in a period of 15 years. In case 1, the reservoir pressure was already at the initial reservoir pressure and a lesser amount of gas was needed to achieve the minimum miscibility pressure. In case 2, the reservoir was already depleted and does not have any potential to produce further oil. Thus, a large amount of gas was required to achieve the minimum miscibility pressure. The results

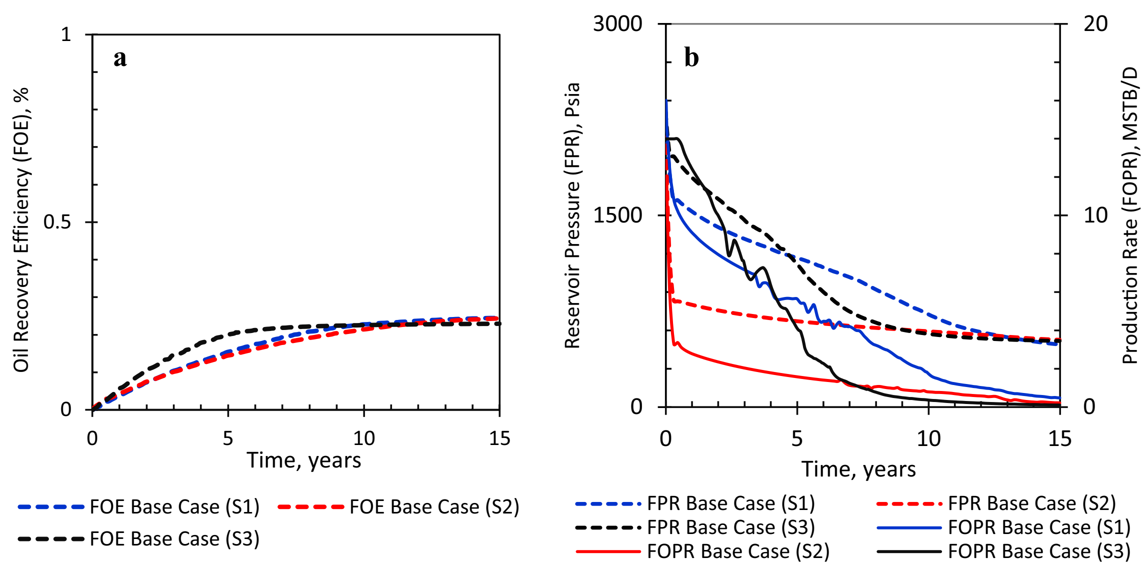

Fig. 9 **a** Oil recovery efficiency, **b** Production rate and reservoir pressure against time in the base case model

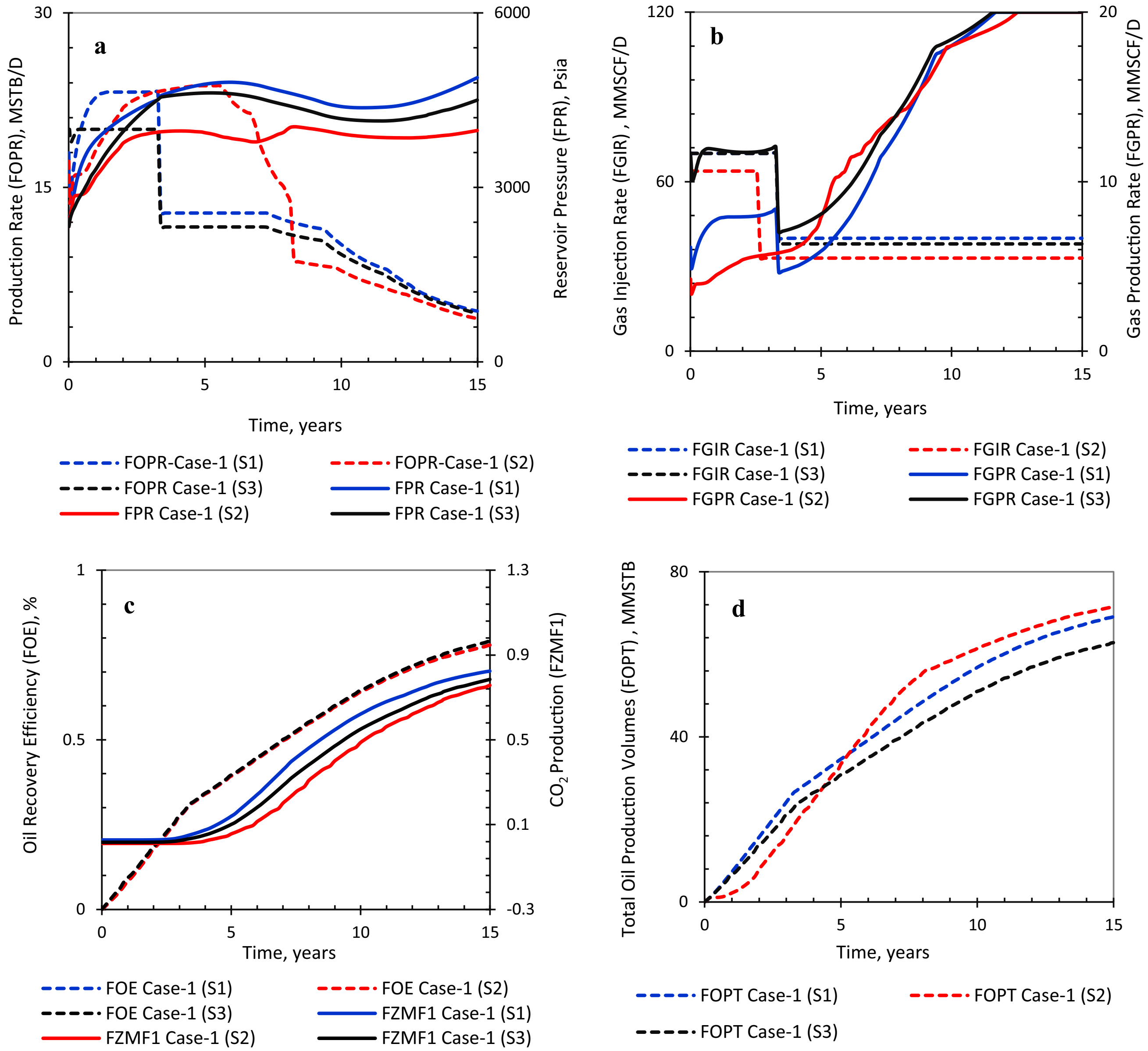

Fig. 10 Comparison between **a** FOPR & FPR, **b** FGIR & FGPR, **c** FOE & FZMP, and **d** FOPT of S1, S2, and S3 samples

obtained are useful to understand the effect of oil type on the performance of the miscible CO_2 flooding.

Conclusions

In this study, a numerical simulation was done to evaluate the performance of the miscible CO_2-EOR in the oil reservoir with different oil compositions. The study results indicated that the miscible CO_2-EOR is perhaps the most suitable technique for the selected fluid samples given the improvement in the oil recovery. It was also found that the fluid composition would affect the recovery performance of the miscible CO_2-EOR. MMP calculation in a similar condition for all three oil samples showed that the MMP increases with the increase in C_1 and C_{5-7+} components and decreases with the increase in C_2–C_4 components. The miscible front in the case of volatile oils is much stable than the heavy oils

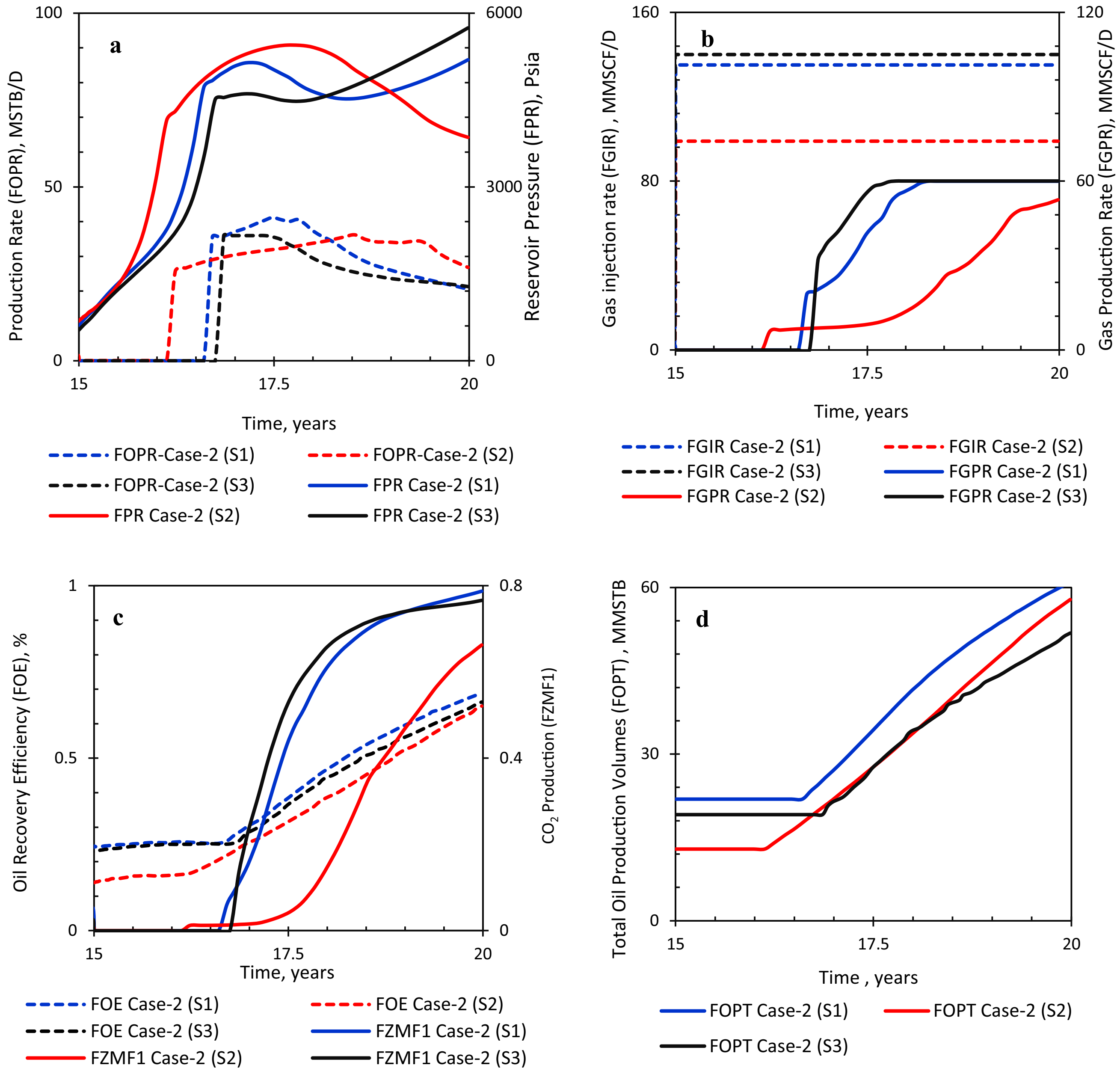

Fig. 11 Comparison between **a** FOPR & FPR, **b** FGIR & FGPR, **c** FOE & FZMP, and **d** FOPT of S1, S2 and S3 samples

due to the lower mobility of heavy oils. The results obtained indicated that the reservoir with the fluid sample S2 would be the most suitable choice for the miscible CO_2 flooding if the recovery factor is counted together with the total amount of CO_2 injected and produced. It was also found that the ultimate recovery increases in a short time period by injecting CO_2 at the miscible conditions from the very first day of production.

Table 4 Results for base case, case 1, and case 2

Cases	Samples	Total oil production (MMSTB)	Total oil recovery (%)	Total gas injected volume (MMscf)	Total CO_2 production (%)	Simulation time (years)	Injection period (years)
Base	S1	22	24	–	1	15	–
	S2	20	24	–	1	15	–
	S3	19	23	–	1	15	–
1	S1	70	78	599	82	15	15
	S2	71	78	495	78	15	15
	S3	62	79	569	79	15	15
2	S1	61	69	2697	79	20	05
	S2	58	65	1978	66	20	05
	S3	52	66	2797	77	20	05

References

Abbasi S, Tavakkolian M, Shahrabadi A (2010) Investigation of effect of gas injection pressure on oil recovery accompanying CO_2 increasing in injection gas composition. In: Nigeria annual international conference and exhibition. Society of Petroleum Engineers

Bachu S (2016) Identification of oil reservoirs suitable for CO_2-EOR and CO_2 storage (CCUS) using reserves databases, with application to Alberta, Canada. Int J Greenh Gas Control 44:152–165. https://doi.org/10.1016/j.ijggc.2015.11.013

Baker L (1988) Three-phase relative permeability correlations. In: SPE enhanced oil recovery symposium. Society of Petroleum Engineers

Bhatti AA, Raza A, Mahmood SM, Gholami R (2018) Assessing the application of miscible CO_2 flooding in oil reservoirs: a case study from Pakistan. J Pet Explor Prod Technol 9(1):685–701. https://doi.org/10.1007/s13202-018-0504-x

Chen P, Kalam MZ, Al Kindi S, Abolhag YH, Shtepani E (2018) Maximize EOR potential by optimizing miscible CO_2 injection parameters in carbonate reservoirs. In: Offshore technology conference

Chen P, Selveindran A, Kumar C, Saloma Y, Bose S, Balasubramanian S et al (2019) CO_2-EOR and carbon storage in indian oilfields: from laboratory study to pilot design. In: SPE western regional meeting. Society of Petroleum Engineers

Choubineh A, Helalizadeh A, Wood DA (2019) The impacts of gas impurities on the minimum miscibility pressure of injected CO_2-rich gas–crude oil systems and enhanced oil recovery potential. Pet Sci 16(1):117–126. https://doi.org/10.1007/s12182-018-0256-8

Gao C, Li X, Guo L, Zhao F (2013) Heavy oil production by carbon dioxide injection. Greenh Gases Sci Technol 3(3):185–195

Huang E (1992) The effect of oil composition and asphaltene content on CO_2 displacement. In: SPE/DOE enhanced oil recovery symposium. Society of Petroleum Engineers

Izgec O, Demiral B, Bertin HJ, Akin S (2005) CO_2 injection in carbonates. In: SPE Western Regional Meeting, 30 March–1 April, Irvine, California. Society of Petroleum Engineers, pp 1–9

Kurdi M, Xiao J, Liu J (2012) Impact of CO_2 injection on condensate banking in gas condensate reservoirs. In: SPE Saudi Arabia section young professionals technical symposium. Society of Petroleum Engineers

Mangalsingh D, Jagai T (1996) A laboratory investigation of the carbon dioxide immiscible process. In: SPE Latin America/Caribbean petroleum engineering conference. Society of Petroleum Engineers

McCain WD (1990) The properties of petroleum fluids. Penn Well Books, Penn Well Publishing Company, Tulsa, pp 1–500

McCain WD Jr (1994) Heavy components control reservoir fluid behavior. J Pet Technol 46:746–750

Muggeridge A, Cockin A, Webb K, Frampton H, Collins I, Moulds T et al (2014) Recovery rates, enhanced oil recovery and technological limits. Philos Trans R Soc A Math Phys Eng Sci 372(2006):20120320

Nasir F, Amiruddin NA (2008) Miscible CO_2 injection: sensitivity to fluid properties. In: SPE Asia pacific oil and gas conference and exhibition. Society of Petroleum Engineers

Orr FM, Heller JP, Taber JJ (1982) Carbon dioxide flooding for enhanced oil recovery: promise and problems. J Am Oil Chem Soc 59(10):810A–817A

Raza A, Gholami R, Wheaton R, Rabiei M, Rasouli V, Rezaee R (2019) Primary recovery factor as a function of production rate: implications for conventional reservoirs with different drive mechanisms. Energy Sources Part A Recovery Util Environ Effects. https://doi.org/10.1080/15567036.2019.1576073